

# Weight Block Sparsity: Training, Compilers, and Accelerators

P. D’Alberto, T. Jeong, A. Jain, S. Manjunath, M. Sarmah, S. Hsu, Y. Raparti, N. Pipralia

**Abstract**—Inference is synonymous of performance. The inference time is how long it takes a forward propagation of a neural network. As faster and tailor-made chip-lets are deployed in the field, larger and larger models are dominating the public’s attention: quantization and sparsification are used to fit these large models into more reasonable sized architectures. Quantization reduces the foot print per model weight and sparsification trims superfluous ones. We present the main ideas about a vertical system where convolution and matrix multiplication weights can be trained to exploit an 8x8 block sparsity and compilers recognize such a sparsity for both data compaction and computation splitting into threads.

Such blocks fully take advantage of both spatial locality that a vector operation can use and temporal locality for reuse and, thus, cost amortization. If we take a Resnet50, we can reduce the weight by half with little accuracy loss. We can achieve speeds of Resnet25. We shall present performance estimates with accurate and complete code generation for a small and efficient set of AIE2 (Versal FPGAs).

**Index Terms**—AI, FPGA, Performance, Sparsity, and Tools

## I. INTRODUCTION

Let us begin by defining block sparsity and a vertical solution. Block sparsity is an intuitive concept, but it is also a little misunderstood. Take a matrix multiplication in Equation 1,

$$\begin{pmatrix} C_0 & C_1 \\ C_2 & C_3 \end{pmatrix} = \begin{pmatrix} A_0 & A_1 \\ A_2 & A_3 \end{pmatrix} \begin{pmatrix} 0 & B_1 \\ B_2 & 0 \end{pmatrix} \quad (1)$$

This is simply the computation:

$$C_0 = A_1 B_2; C_1 = A_0 B_1; C_2 = A_3 B_2; C_3 = A_2 B_1 \quad (2)$$

and in general with proper  $\gamma_i$  (i.e., a mask):

$$C_i = \sum_{k=0}^1 A_{2i+k} (\gamma_{2*k+i} B_{2*k+i}) \quad (3)$$

Where the matrix  $B$  is constant, diagonal, and each submatrix  $B_2$  and  $B_1$  can split further down and may have even smaller zero blocks. In this work, we chose the basic block of  $B_i = 8 \times 8$ . It is a great starting point for architectures based on AMD AIE2 products and we support others (see the hardware abstraction Section IV-A for an explanation why the  $8 \times 8$  is, for lack of better words, good). For example,

$$B = \sum_i \gamma_i B_i, \quad \gamma_i \in \{0, 1\} \quad (4)$$

Each block is a constant either non-zero or zero:

$$B = \begin{bmatrix} \gamma_0 B_0 & \dots & \gamma_0 B_{n-1} \\ \gamma_n B_n & \dots & \gamma_{2n-1} B_{2n-1} \\ \dots & \dots & \dots \\ \gamma_{(n-1)n} B_{(n-1)n} & \dots & \gamma_{(n-1)^2} B_{(n-1)^2} \end{bmatrix}$$

Of course, the matrix  $A$  does have any value and so does  $C$ . Some applications have some constraints about the row and columns of  $B_i$ , for example, all the values in each row or column cannot be zero. In practice, we do not prune the network, we keep the same number of *channels* everywhere.

This is a well-known data structure in the sparse computation field: We can use *compress block row* (CBR) or *column* format (CBC). There are standard Matrix Sparse-Matrix Multiplication interfaces and algorithms for CPU and GPUs using this data format (where only one operand is sparse or both).

In the CBR format, the  $\gamma_i$  are not present and only non-zeros elements are stored [1], [2]. In other architectures, we can choose to store all non-zero blocks in row format and keep a matrix  $\Gamma$  of zeros and ones (or columns). The  $\Gamma$  is a bit matrix (here) but it can be represented as a short integer matrix representing the non-zero block column.  $\Gamma$  is two orders of magnitude ( $8 \times 8 \times 4$ ) smaller than the sparse or original  $B$  matrix. We are working with *human-made* block sparsity and the block is a property of the hardware.

In classification, the model weight size determines one important aspect of the model complexity: the number of operations per single output, the relation between layers (e.g., depth), and redundancy. In our context, sparsity is the zeroing of weights (convolution and fully connected). We start with dense models using full precision and we must find a way to choose the binary matrix  $\Gamma$ , the mask. For a matrix multiplication the mask is  $\Gamma \in \mathbb{R}^{n \times m}$ . In a convolution,  $n$  is the number of output channels (divided by 8) and  $m$  is the number of input channels (as above) and each  $B_i \in \mathbb{R}^{8 \times h \times w \times 8}$  where  $h$  and  $w$  are the height and width of the convolution kernel.

We explore training techniques (PyTorch, Keras is available in GitHub) with the most successful being the most straightforward. We take a pre-trained model, compute a  $\Gamma$  per layer using a function to determine the blocks more likely to be zeros (Norm), and train the model until convergence or accuracy is achieved. We take the sparse model and quantize to 8-bit integer computations by using the Vitis-AI quantizer. The final model is a AMD/Xilinx IR (XIR) quantized model. See the training Section III.

For the FPGA accelerator using AIE2, we have a custom compiler that takes the XIR model and an abstraction of a connected set of AIE2. See the compiler Section IV. For example, a DDR, one or two memory dedicated per column (512 KB each) called **memtile**, short for memory tile, 1 to 8 columns, 1 to 8 AIE2 cores per column, and each core has 8

banks of 8 KB internal memory (64 KB). There are vertical connections and there are horizontal connections. Given the HW and per layer, the compiler computes the maximum sub-volume computation per core. By heuristics and following a schedule, it computes a memory allocation in memtile for input, outputs, and weights. It formats the weights so that to exploit spatial distribution to memtiles and cores into a single compacted tensor.

With the schedule and the DDR-memtile allocation, we generate all the explicit communications between DDR, memtile, and cores. Knowing the subproblem sizes per core and the computation throughput, and with a clear specification of what is executed in parallel, we can estimate the execution time per layer and of the entire network with an accuracy closer to a simulation.

When the code is valid, the native AIE2 compiler can interpret it with all the DMA settings in place. This was tested for a single core in HW. We will use this code to have a detailed time estimate for all parts of the computation that show estimates for two CNN models and a few different AIE designs (see Section VI-A).

In Section II, we start with a quantitative measure about the advantages of block sparsity.

## II. BLOCK-SPARSE MATRIX-MATRIX MULTIPLICATION

As a mental and practical exercise, consider  $\Gamma$  and  $\Omega$ , two appropriate 0,1 matrices for square matrices in  $\mathbb{R}^{N \times N}$

$$C = (\Gamma A) * (\Omega B) \quad (5)$$

More precisely, consider non-zero blocks of size  $k \times k$  so that

$$C_{i*N+j} = \sum_k (\gamma_{i*N+k} A_{i*N+k}) (\omega_{k*N+j} B_{k*N+j}) \quad (6)$$

Thanks to the sparsity and if we store only non-zeros, then  $\gamma_{i*N+k}$  is at the very least contiguous but  $\omega_{k*N+j}$  and the right operand accesses are far from being neither simple nor contiguous.

$$\Omega \dot{B} = (\Omega B)^t = \Omega^t B^t \quad (7)$$

Although expensive, the transposition of a sparse matrix is a sorting algorithm. We start from a row order and we go to a column order, then considering  $K$  non-zeros, we have  $O(K \log_2(K))$ .

$$C_{i*N+j} = \sum_k (\gamma_{i*N+k} A_{i*N+k}) (\dot{\omega}_{j*N+k} \dot{B}_{j*N+k}) \quad (8)$$

There will be a meaningful product to compute if and only if  $\gamma_{i*N+k} = 1$ ,  $\dot{\omega}_{j*N+k} = 1$ , and  $k_\gamma = k_\omega$ . Then we merge-sort these vectors only on equality  $k_\gamma = k_\omega$ . If you like to break codes yourself, see how the sparse sparse matrix multiplication using coordinate block structure (COO), see [3]. We have a parallel sorting and a parallel matrix multiplication.

Now, the quantitative part, assume we want to achieve a fixed sparsity (i.e., density) of 50% for a square matrix of size  $N$  and we choose the block size  $k \times k$ . The number of blocks per dimension and thus the overhead for sparsity and sorting,

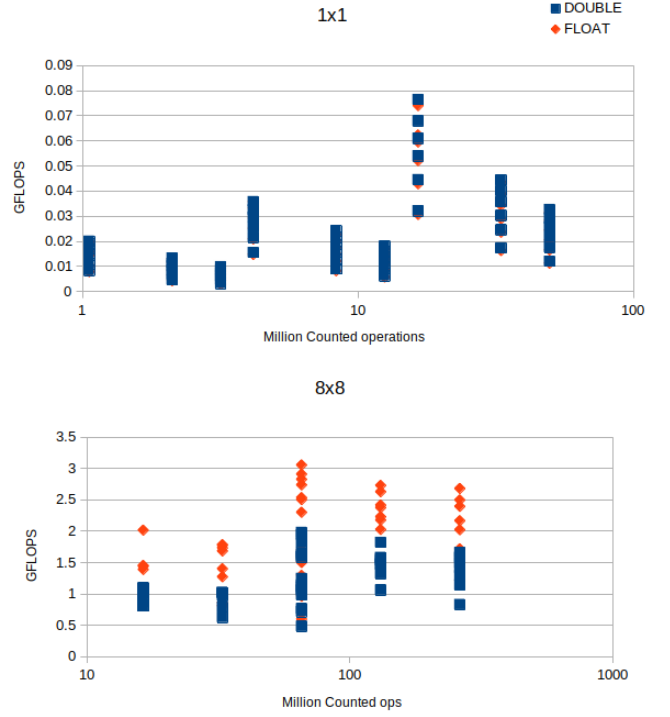


Fig. 1. Block 1x1 and 8x8 performance

is basically  $\frac{1}{2} \frac{N}{k}$ . The larger  $k$  is, the smaller the overhead will be. The relative performance of the  $k^3$  multiplication is better as  $k$  get larger because spatial and temporal locality and optimized code for a constant/parameterized  $k$ .

In Figure 1, we present two scatter plots: on the abscissa the effective multiplication-and-addition number and on the ordinate the performance in GFLOPS when the sparse matrix with dense block is 1x1 and 8x8. Given the same problem, we may use more threads and thus the Jenga of points. We can see that given the same number of effective operations, the block allows better performance and exploits better performance for each precision.

## III. BLOCK SPARSITY: TRAINING AND QUANTIZATION

In Convolutional Neural Networks, the two main operations are convolutions/correlations and fully connected layers (matrix multiplication). The block sparsity we are seeking to deploy is not naturally recurring and we must train the network for it.

First, let us clarify block sparsity for convolution weights, then we can explain our training process and options. A convolution has a weight tensor in four dimension:  $\mathbf{W} \in \mathbb{R}^{c_{out} \times h \times k \times c_{in}}$ . In the hyperplane of the  $h$  and  $k$ , we can simplify the weight as  $\dot{\mathbf{W}} \in \mathbb{R}^{c_{out} \times c_{in}}$  and block sparsity can be simply described by a mask  $\Gamma \dot{\mathbf{W}}$ . Although, we speak of a  $8 \times 8$  of non-zeros, this is in practice a  $8 \times h \times k \times 8$  block. For the matrix multiply  $h = k = 1$ , there is no difference from the previous discussions.

### A. Keras

We provide a repository using Keras [4] where we implements the contents of this section: where anyone can reproduce and break [5]. We target convolutions only and without quantization. The idea of the framework is simple by taking any model and creating a copy where we enhance the convolution with a (non-trainable)  $\Gamma$ . A convolution will have three parameters (saving the model into a different format). The forward computation is modified so that the weights used for convolution are  $\Gamma \mathbf{W}$ . We assume the backward computation (i.e., gradient) is done automatically from the forward definition. There is no need to change the bias. For example, we take Resnet50 from the Keras application repository, we start with a  $\Gamma = 1$ , and we trained one epoch using imagenet repository [6]. The goal is to choose  $\Gamma$  so that we achieve the required sparsity and to have the minimum loss in accuracy.

A little notation first. We start from an optimized network and assume a loss function  $\ell(x, w)$ . In a close interval of the optimal solution  $w_0$ , we have:

$$\ell(x, w_0 + \Delta w) = \ell(x, w_0) + \nabla \ell * \Delta w + (\Delta w)^t * H * (\Delta w) + \epsilon \quad (9)$$

Where the gradient of the loss function is about zero and defined as

$$\nabla \ell * \Delta w = \sum_{w_i} \frac{\partial \ell}{\partial w_i} \Delta w_i \rightarrow 0 \quad (10)$$

The second component is the Hessian, it is symmetric and either definite positive or negative as a function of the loss.

$$(\Delta w)^t * H * (\Delta w) = \sum_{w_i} \Delta w_i \sum_{w_j} \frac{\partial \ell}{\partial w_i \partial w_j} \Delta w_j \quad (11)$$

We start from  $w_0$ , the current optimal weight, and we must choose how to reduce to zeros the weights to zeros. In practice, using the code available in [5], we started with an accuracy of 75% top-1 and we ended up with a 68% without accounting for quantization. The investigation using PyTorch [7], after sparsity and quantization, achieves only 3% top-1 accuracy drop (instead of 6+), making the training for sparsity quite worthwhile (Section III-G).

### B. $\Gamma$ Chosen Once and Full Training Ahead

Take a convolution with  $\Gamma = 1$  and weights  $\mathbf{W}$ . For each  $\gamma_i$ , this will be representative of a block  $\mathbf{W}_i \in \mathbb{R}^{8 \times h \times w \times 8} \sim \mathbb{R}^{8 \times 8}$ . We can choose the  $\mathbf{W}_i$  using a measure of importance:

- $L_2(\mathbf{W}_i) = \sqrt{\sum_k w_k^2}$  with  $w_k \in \mathbf{W}_i$ ,
- $L_1(\mathbf{W}_i) = \sum_k |w_k|$  as above,
- Variance  $\sigma^2 = \frac{1}{64} \sum_k (w_k - \mu)^2$  with  $\mu = \frac{1}{64} \sum w_k$  with  $w_k \in \mathbf{W}_i$  or  $\frac{1}{N} \sum w_k$  with  $w_k \in \mathbf{W}$  (the full tensor). In signal processing  $\sigma^2$  is the power of the signal.

We can then sort them in ascending order and for example choose the first 50% to set to zero. Then we start re-training. We do this for the entire network or for one convolution at a time. This is the approach used in Section III-G.

### C. $\Gamma$ Chosen in Steps and Small Fine Tuning

For example, for every convolution,  $n_i = \sum \gamma_i$ , which is the number of blocks, reduce this number to  $\frac{n_i}{2}$ . For each epoch (say every two training epochs), we consider the current non-set-yet mask elements  $\sum (1 - \gamma_i) = k < \frac{n_i}{2}$ . We compute our importance measure for all in ascending order. This time, we zero the first  $\min(\frac{5}{100}k, 1)$ . We keep this process until we reach 50% sparsity. At each iteration at least one block will be set to zero. We trace a solution path as much as geodesic as possible.

### D. $\Gamma$ Trainable as Optimization Problem

If we want to make  $\Gamma$  part of the optimization process as trainable variable we could introduce a penalty function into the loss  $\ell(x, w) + \lambda(w)$ . First let us introduce an approximation for the  $\max(x)$ , so when in this section you will read  $\max, \min$ , this is a log sum expontial, which is continuous, derivable everywhere, and convex:

$$\max(x) = LSE(x, \alpha) = \frac{1}{\alpha} \log \sum e^{x_i * \alpha} \quad (12)$$

With  $T$  we represent the number of non-zero block in  $\Gamma$

$$\lambda = -(\max(\Gamma) - \min(\Gamma)) + \beta * L2(\Gamma - T) + \iota * L1(\Gamma) \quad (13)$$

This is a simplified loss so that we minimize the value of  $\Gamma$  but also try to maximize the difference of the elements.

$$\lambda = \max(-\Gamma, 0) + \max(\Gamma - 1, 0) - (\max(\Gamma) - \min(\Gamma)) + \beta * L2(\Gamma - T) + \iota * L1(\Gamma) \quad (14)$$

This last penalty function represents our attempt to state that the  $\gamma_i$  should be positive and in the interval  $[0, 1]$  and in a such a way that we maximize the distance of the elements between 0s and 1s.

$$\lambda = \max(-\Gamma, 0) + \max(\Gamma - 1, 0) - \frac{\min(\Gamma)}{\max(\Gamma)} + \beta * L2(\Gamma - T) + \iota * L1(\Gamma) \quad (15)$$

We can exploit this functionality in Keras. The penalty function can be added easily and per convolution (if you like) and it is available in the code reference. We could not use it successfully.

### E. Hessian and Fisher Information

If we have  $N$  parameters/weights, the Hessian  $H \in \mathbb{R}^{N \times N}$  has quite the space complexity (consider even small models could have million parameters). When we are already close to the optimal solution or we are trying to move from the optimal solution without using information from the gradient, the Hessian provides the most information close by an already established solution point. There are also ways to compute the Hessian and the effects of the Hessian by using Fisher information [8]–[10]. This will reduce to the computation of the gradient of the loss function.

### F. Diagonal Hessian

We applied a Fisher measure and computed  $\nabla^2 \ell$ , that is computed just the diagonal of the Hessian. Again, we use the  $L_2$  over the normalized weight and went through the process of training. The elements of the diagonal are not representative in general, but they are a good approximation of the contribution of a single weight. The Fisher and  $\nabla^2 \ell$  did not provide any main advantages. But this information is very useful in quantization and optimizations within the same field and application.

### G. PyTorch

In Table I, we show the results by using one-time masks and full training: VGG-16, ResNet-50, Inceptionv3 on ImageNet20 (20 classes), and ImageNet1k (1000 classes). See Section III-B. We use three samples per class for the validation accuracy for ImageNet1k data set. Instead, we use 50 samples per class for ImageNet20. Fine-tuning sparse networks on the original ImageNet data-set [6] is expensive. To reduce the training time, we chose 20 classes (from the original 1000 classes) with the least number of images per class in the training data-set and this choice will affect the accuracy because there are fewer sample for re-training.

TABLE I  
ACCURACIES OF THE SPARSITY MODELS

Model	Dataset	Baseline Acc.(%)	Sparsity		Acc.(%)
			block	ratio (%)	
Inception-v3	ImageNet1k	77.2	8x8	50	75.5
ResNet-50	ImageNet1k	76.7	8x8	50	74.6
VGG-16	ImageNet1k	70.6	8x8	50	69.7
ResNet-50	ImageNet20	96.1	8x8	25	95.1
ResNet-50	ImageNet20	96.1	8x8	50	92.0
ResNet-50	ImageNet20	96.1	8x8	75	87.1
ResNet-50	ImageNet20	96.1	1x1	25	96.0
ResNet-50	ImageNet20	96.1	1x1	50	95.6
ResNet-50	ImageNet20	96.1	1x1	75	93.5
VGG-16	ImageNet20	92.0	8x8	50	89.6
VGG-16	ImageNet20	92.0	1x1	50	92.3
VGG-16	ImageNet20	92.0	1x1	75	91.7

Classification accuracy on ImageNet1k drops by only 1 - 2% after applying 50% sparsity with a  $8 \times 8$  block (this is without any quantization). We experiment with different block shapes such as  $16 \times 4$  and  $4 \times 16$  on ResNet-50, but the accuracy is slightly worse compared to block of  $8 \times 8$ . Fine-grained sparsity ( $1 \times 1$  block) does not sacrifice any accuracy (i.e., almost any). We use the sparsified Resnet50, we quantized using Vitis AI. Then we will use it to estimate the time advantages (i.e., Section VI-A).

## IV. COMPILER AND ITS CODE GENERATION FOR AIE

Within our AMD effort, we can take a PyTorch/Keras model, quantize it using Vitis AI, and create an intermediate

representation that we call the Xilinx Intermediate Representation (XIR). This is a graph where each node is an operation that reads tensors and writes one tensor. A convolution has one quantized input. We use the tensor layout format BHWC. The tensors are represented in INT8 with a position where the fraction starts (power of two scale). It computes a tensor using the same layout as the input and with a proper scale. The weights and bias are properties of the convolutions, as such they can be tailored; the layout of the weight tensor is  $COUT \times h \times w \times CIN$ , which is similar to the caffe layout [11] (different from [12]).

For this project, we are at the third generation of a compiler for custom architectures (previously DPUV1 and DPUV3int8 [13], [14]). The main common hardware feature for this new architecture is the availability of two main memory levels: DDR and memtile. For such memory, we import the philosophy of memory data layout and memory allocation (of the previous compilers). The main difference is the ability to represent a parameterized block sparsity (block size and overall sparsity ratios) and the capability to split these tensors when we split the computation.

All weights are statically prepared into DDR and we move them explicitly towards the inner levels. Inputs and outputs have designated space in DDR (to communicate externally with PCI connection or RAM). DDR can and will be used for swap tensors in case the inner levels do not allow allocation. The compiler can explore different schedules. The memory allocation to memtile is basically coloring algorithms and some heuristics. In this architecture, we do not allow *streaming* of neither data nor weights (because they share space in memtile). In a previous architecture, that was possible.

### A. AIE Hardware Abstraction

For this presentation, see Figure 2, we work with a mesh of  $4 \times 4$  AIE2 cores connected by four horizontal and four vertical interconnections (we shall presents estimates for square  $2 \times 2$ , ..  $i \times i$  ..  $8 \times 8$  and rectangular shapes are in the works). Each core has eight banks memories for a total 64KB. About six banks are used as input/output/weight buffers and two banks are used as temporary space for kernels. Each core can request and send data to its direct neighbors (if aware of connection and control). Double buffering as ping/pong is commonly used for inputs and outputs.

The AIE2 is a large DSP. It can perform  $8 \times 8 \times 4$  multiply-addition in a single cycle using INT-8 operands and INT-32 accumulator (integer with 8 bits and 32 bits respectively). The above granularity dictates the sparsity block size of  $8 \times 8$ . This means, we can manage the AIE2 full throughput with enough data per block and easily skip non-zero computations without loss of performance. We do not investigate nor try pruning the input tensor communication.

There are four memtiles, where each 512 KB can either be connected to one columns and its direct neighbor column, or it can be connected to a row and its neighbor. The total amount of space is 2 MB. Memtile is a circular buffer to exploit more

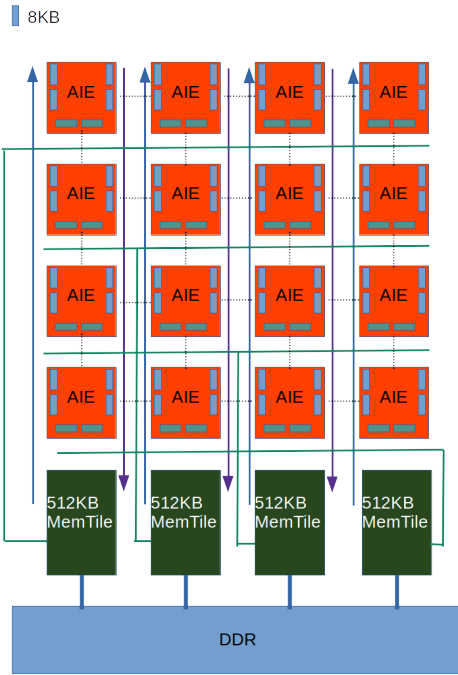


Fig. 2. 4x4 AIE representation

flexible allocation, implicitly a  $2 \times 2$  architecture will have one memtile per column and a total of two (1MB).

A memtile can broad-cast data per column or per row. We can dedicate a memtile for weights, one for activations, or we can share. We will show mostly shared configurations. To maximize the computation parallelism, every core will write data per column into memtile where there are different designs that can be used. We will explore the case where Inputs/Outputs/Weights are evenly distributed across memtiles although the distribution is different per tensor.

The DDR is connected with two channels to write into each memtile and each memtile can use two channels to write into DDR. DDR and memtile communications are parallel. The abstraction can be extended to more complex connections (from  $1 \times 1$ ,  $8 \times 2$ , to  $8 \times 8$  and more rows of memtiles designed for larger chips). But  $4 \times 4$  is representative for the AIE engines you will find in the next generation of CPU+FPGA chips.

### B. Sub Volume, Data Compression, and Data Movement

There are a few assumptions we would like to clarify. The computation is split by column. Each output tensor is split evenly by width, so each memtile will store different columns by width. Each core will compute different output channels, and the computation streams computing the height of the tensor by using core input and output ping/pong. As often as possible, we store the weights in the core and we reuse them as much as possible (unless we need to stream the weight instead). The set of cores is a cohort and symmetric computations are always selected. This means that we do not merge two operations like convolution and max-pool and give

three columns to convolution and one column to max-pool. Other approaches in the literature are more advanced.

Before we start describing the memory allocation, we have to explain and compute the size of the sub-volume computation at the AIE core. That is, if we have the inputs, output, and weights in memtile, what is the largest computation we can do in the AIE? The minimum computation is at least one output channel and one row by height. If this is not possible, we try to reduce the size of the width (e.g., shaping the tensor in memtile by using DDR spills so that one row of data is smaller) and we can manage to split the input channels (this will require to split the weights accordingly and accumulate). We call W-Split the distribution of tensor by columns in the AIE mesh. We can COUT-split, this will require the partial transfer of weights (but we can stream by height). We can CIN-split when we need to split by input channel, this is the last resort because it is also the most expensive (accumulation of the outputs and no streaming). Once we have the subvolume, we know if input and output tensor need W-split or CIN-split. This means that the tensor cannot fit completely in memtile and part of it will be moved. Or the computation will need to read from memtile the same inputs or weights multiple times.

At this stage, the subvolume describes the smallest shape of the weights we need to manage. We compress the weight accordingly to a subvolume so that any data movement will always be a multiple of the subvolume and can be a single load. Such a compress data will have the same properties whether it is sparse or dense. Of course, sparse data is smaller and we compute fewer operations.

1) *Hidden Problems:* This and the next section are parenthetic sections about the problems related to sparsity, subvolumes, and practical communications, when we perform CIN-split. You may skip, if you find the problem of splitting sparse tensors too abstract at this time. When we take a convolution and its weights  $\mathbf{W} \in \mathbb{R}^{m \times n}$  where  $m$  and  $n$  should be multiplied by eight to describe the real sizes. Assume we must split the computation by  $m$  into four buckets. If  $\mathbf{W}$  is dense, then we can just take the tensor and split into four slices of size  $\lceil \frac{m}{4} \rceil$ . The first problem is to realize how we split the computation when  $m \bmod 4 \neq 0$ . The second problem arises when we introduce sparsity. Consider the case when a row of  $\mathbf{W}$  is 50% sparse and this is the only constraints. This is no different from the dense. We can split evenly the problem because the same sparsity applies to all rows. Now, consider that the sparsity is by column: we take a column of  $\mathbf{W}$  and 50% are zeros in any order. When we must split by  $m$ , by row, there is no assurance of evenly distribution. The worst case, two components with only zero elements each and the others have the rest. This happens when the convolution is large and the only way to split the problem is by input channels (CIN-split). There are interesting solutions for this scenario.

2) *Hidden Solutions:* First, when we have the list of convolutions and the HW abstraction, we can check if we need COUT-split or CIN-split (the compiler does a pass and annotates every layer with CIN-split information). We can train sparsity for one or the other. For the CIN-split sparsity

we assure that the column has 50% sparsity and thus we can evenly split the problem. This training is possible and the compiler will prepare all the data structures. By default, the training and the data structure support COUT-split (the compiler will have to deal CIN-split unbalance as below).

Second, we do bookkeeping and we create an unbalanced collection of subvolumes, create the proper bit maps, and data structures. There is a clear advantage: we transmit only the data needed. There are two disadvantages: asymmetric communications and computations. The communications at this level (memtiles) are parallel, but the dominant subgroup will dominate. We save energy and there is a cost. AIE2 cores will have different work to do complicating the synchronization across cores and columns. The most sensible choice is the padding with zeros of the smallest subgroup so that to have a symmetric distribution of weights.

The compiler profiles the sparsity per COUT and CIN split. It creates a tree where it stores the number of subvolumes for each COUT-and-CIN partitions. Then, if necessary, the compiler stores the weights so that each subproblem is contiguous but separated. There is only one load per subgroup and per memtile.

### C. Schedule and Memory Allocation

This is a two level memory hierarchy. During the scheduling of each layer, we evaluate what can fit in mem tile. Here, activation and weight tensors share the space. It means that an input tensor is distributed among the memtiles identified by one starting address and a final address and weights are distributed similarly. At each step the memory allocation will check if we can allocate a tensor in memtile. If we cannot, we evict all tensors by moving them into DDR and then split/time the computation.

At the end of this stage, every tensor will have an address in memtile or DDR (or both). When we reach a layer in the schedule, it has only DDR addresses, the compiler the layer and its context and, by heuristics, will split the layer computation (thus the output tensor) by width, output channel, height, and input channel (no necessarily in this order). Every computation will have the DDR to and from memtile and its data movements for the first two levels of the memory hierarchy. The heuristics have a simple objective. Find the largest problem fitting the memory level with the assumption that the output tensor will be built by row and streaming using ping/pong double buffering (considering padding, strides and kernels sizes).

We use an implementation that takes a recursive approach in tiling [14]. For clarity,  $\sum$  is a parallel loop and a W-split can be written as

$$Y = Conv(X, W) = \sum_w Conv(X_w, W) \quad (16)$$

The split is pre-computed as function of the foot print, before and after each convolution there will be an explicit data movement. At this stage each input, output, and weights will have an address associated with each sub-computation. Consider a subcomputation as data movement, computation, and data

movement. Data movements are optional or decorators. The code generation of each  $Conv(X_w, W)$  is independent and, recursively as needed. There will be specific splits of the computation accordingly. This is a tree (i.e, a root with  $k$  children). Sub-convolutions may have different memory requirements, so we try as much as possible to obtain symmetric computations (some columns will have to compute slightly larger than needed tensors). If the convolution has strides and large kernel, each sub-convolution will have overlap data but defined addresses and data movement if necessary. For example, computing the output by rows and the weights are reused.

$$\forall w, Conv(X_w, W) \rightarrow \sum_h Conv(X_{w,h}, W) \quad (17)$$

### D. Code Generation

The compiler recursively creates a list of operations smaller and smaller that can actually be executed memtile to memtile. In practice, there is a further decomposition using only AIE cores but it is completely determined by the subvolume computation as we explained previously. Then, we can explicitly determine the data movements from memtile to core and back. Here, we will show how we produce the execution time estimates in Figure 3 or 4. Do not adjust the paper. On the vertical line there is time in seconds and it evolves by going up (if you flip, it goes from left to right). On the horizontal line, there are the instructions separated to create a sequence of time series. We will explain further in the next sections.

An important feature of the current system is the concept of **iteration**, using locks and chaining them (locks like in semaphores). We can write a single instruction from the prospective of a single core (as a SIMD instruction) but driving all cores at once (ASM-like code) for multiple iterations:

```
LOADFM Lock k_0 memtile addr core addr iter i
CONV iteration i
WRITEFM Lock k_1 memtile addr core addr iter i
```

There is an implicit lock (say  $k_x$ ) that is used for the pong and the system cycles in between locks ( $k_x$  and  $k_0$ ). These three operations will execute a number of iterations  $i$  and using a ping/pong they will load different slices of data and compute different slices of data. The key ingredient for this to work is the volumes of input and output tensors are all the same. In our environment, padding is common and we can manage with a custom load (from memtile to core). This requires a custom load that will not be repeated.

```
## Head top padding < 50 us First comp block
LOADFM Lock k_0 memtile addr_0 core addr iter 1
CONV iteration 1
WRITEFM Lock k_1 memtile addr_1 core addr iter 1
## Body iteration > 50 us < 150 us
## k_0 -> k_2 -> k_4 Lock Chain
LOADFM Lock k_2 memtile addr_2 core addr iter 9
CONV iteration 7
WRITEFM Lock k_3 memtile addr_3 core addr iter 9
## tail > 150 us Last computation block
LOADFM Lock k_4 memtile addr_4 core addr iter 1
CONV iteration 1
WRITEFM Lock k_5 memtile addr_5 core addr iter 1
```

See Figure 4 for how this code will function in practice. At this stage we have all the information. Per layer, the code



Fig. 3. Resnet50 for 4x4 AIE with dense weights

generation is a two pass process. First, we generate code for the all load/store. Second, we combine them into chain having dependency so that it is logically correct and as fast as possible.

#### E. Time Estimation

At this stage, we need to explain how we can capture the execution time and visualize it as in Figure 3.

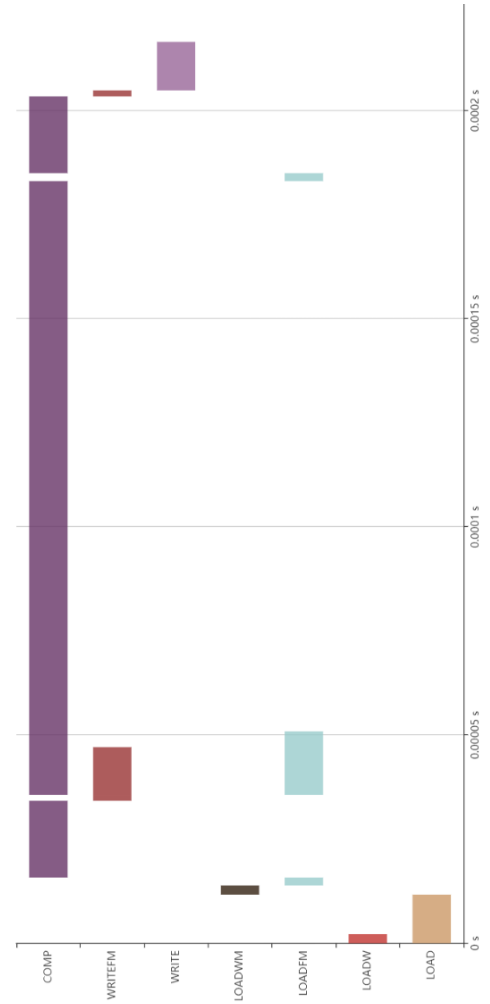


Fig. 4. Resnet single convolution with padding for 4x4: legend AIE: LOAD Activation DDR to Memtile, LOADW weights DDR to Memtile, LOADFM Activation Memtile to AIE2 cores, LOADWM weights Memtile to AIE2, WRITE Memtile to DDR, WRITEFM AIE2 to Memtile, COMP Computation

#### F. Time estimates for DDR to Memtile

We have two communication types: activations and weights. Per memtile there are two dedicated channels.

- If we share activations and weights in the same memtile, we can use one channel for activations and one for weights. Thus, the loads from DDR to memtile (LOAD and LOADW) are parallel with a bandwidth of 4 GBps. Writes from memtile to DDR (WRITE) can use both channels (8 GBps). We will expand this.
- If activations and weights go to different memtiles (2 and 2), each load is parallel and 8 GBps. Writes are identical.

First, when we share weights, they must stay still to be reused. If weights are not shared, then in general inputs and outputs have different rates of consumption and hence, one will overwrite the other. Ping/pong techniques will decrease the space available, but it will hide latency. Currently, we will try to increase the reuse.



### G. Time Estimates for Memtile to AIEs

The memtile connections with AIE cores can be designed differently. We assume a few channels with 4 GBps bandwidth. One memtile can broadcast inputs to a cores column (and to the nearest neighbor). These communications are for activations (LOADFM). One memtile can broadcast to rows of cores (or the nearest neighbor), these are for weights (LOADWM). We assume that the column and row communications are parallel and each memtile core connection is parallel.

Every communication with iteration 1 is synchronous and binding. That is sequential, the load, convolution, and store is one after the other and every core is independent. For synchronization and for bookkeeping, we assume that AIE2 weights communication (from memtile) to core are synchronous and halting.

Every communication with iteration larger than one, we assume that load, computation (COMP), and store (WRITEFM) are executed in parallel and the overall execution time is the maximum of the estimated time multiplied by the number of iterations.

We estimate the execution time of a subvolume by the number of operations divided by the maximum number of operations per cycle which is in our scenario:  $4 \times 8 \times 8 = 256$  operations per cycle and 1 GHz frequency. This is a very optimistic validation and not only for convolutions (asking for a ratio of 1 in efficiency), but also for operations like average pools and element-wise additions. The execution time is a feature of the analysis but for us the estimate of the communications is more compelling and we can easily mute the computation contribution.

We do not account the wait and synchronization which are necessary to reprogram the fabric. These are very expensive running on a few milliseconds.

During and especially once we generated the code for all data movements, data volumes and destinations, the trigger of the computation, and the subvolume per computation, we can estimate accurately the execution time for each operations and account their parallel execution.

### H. Convolution Example

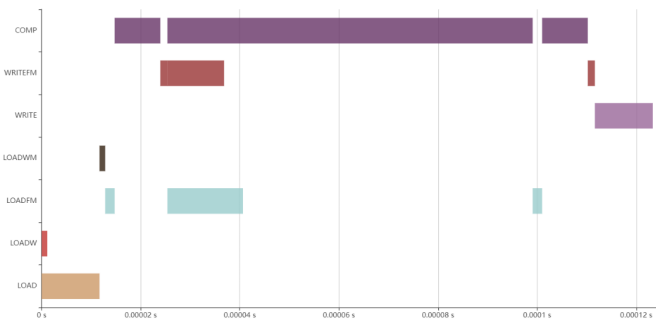


Fig. 5. Resnet single convolution with padding and sparsity for 4x4 AIE

Here and in Figure 4 and 5, we give a full convolution example with and without sparsity and with padding. We can

explain how the time is really estimated and also how the hardware works in principle.

It is clear from the figures above that there are three computations (COMP). We load the weight and activations once in memtiles. There are actually one load per memtile for a total of four loads per activations and four loads for weights. Because each load is to a different memtile, they are parallel. The activation and weights communications are using two different channels and are in parallel with 4 GBps bandwidth.

There is a single load of weights from memtiles to each core. This is done once and it is blocking (LOADWM), but it can be made non-blocking and parallel to the activations. There is a computation using padding (top-padding) and you can see the sequential execution of load to cores (LOADFM), computation (COMP), and write to memtile (WRITEFM). This computation has iteration 1. There are nine iterations for three instructions. We can see the load, the computation, and write in parallel. See Figure 4 for the dense convolution in the time interval between  $20\mu s$  and  $180\mu s$ . This is a simplification. There will be a little load poking out at the beginning and a writing poking out at the end. Then, we conclude with the final computation with padding at the bottom of the computation.

In this particular scenario, the computation dominates the execution time and compression basically cuts the execution time by half: from  $200\mu s$  to  $130\mu s$ . There are convolutions in Resnet that realize up to  $2\times$  performance. There are convolutions that are dominated by the read or by the writing and where sparsity only helps in space saving.

### V. DEPTH-WISE SUBGRAPH TILING

In this section, we introduce an optimization designed to reduce the activation's DDR accesses, which sparsity does not.

Consider a graph and a schedule describing the computation order. For example, the schedule  $L_0, L_1, \dots, L_n$  represents the layer computation order. We compute  $L_i$  once and thus its output tensor  $T_i$ . Multiple layers can read  $T_i$ . Assume, we have a sub-schedule  $L_0, L_1, \dots, L_j$  with  $j < n$  that is a convex subgraph with one input, one output, and every layer spills into DDR. That is, every layer  $L_i$  will have its inputs and its output in DDR. We present an example in Section VI-B. The compiler will apply different types of splitting W-split and H-Split to accommodate data locality per layer into the memory hierarchy. Fusing layers  $L_i$  and  $L_{i+1}$  may exploit better locality of the temporary tensor  $T_i$ . In this case, consider the layers like a single layer, change the schedule, and we proceed. We cannot do better unless we are ready to allow re-computation.

Depth-wise tiling is the idea of tiling the output tensor  $T_j$  into tiles  $u_i$ , then cut the computation accordingly to find the minimum corresponding input shape and size of  $T_{-1}$  and  $T_0$ , even overlapping, to carry the computation to  $u_i$ .

#### A. Generalized Convolution

Take the last layer  $L_j$ ; it has an output tensor  $T_j$  and an input tensor  $T_{j-1}$  (e.g., it can have multiple tensors imagine a layer



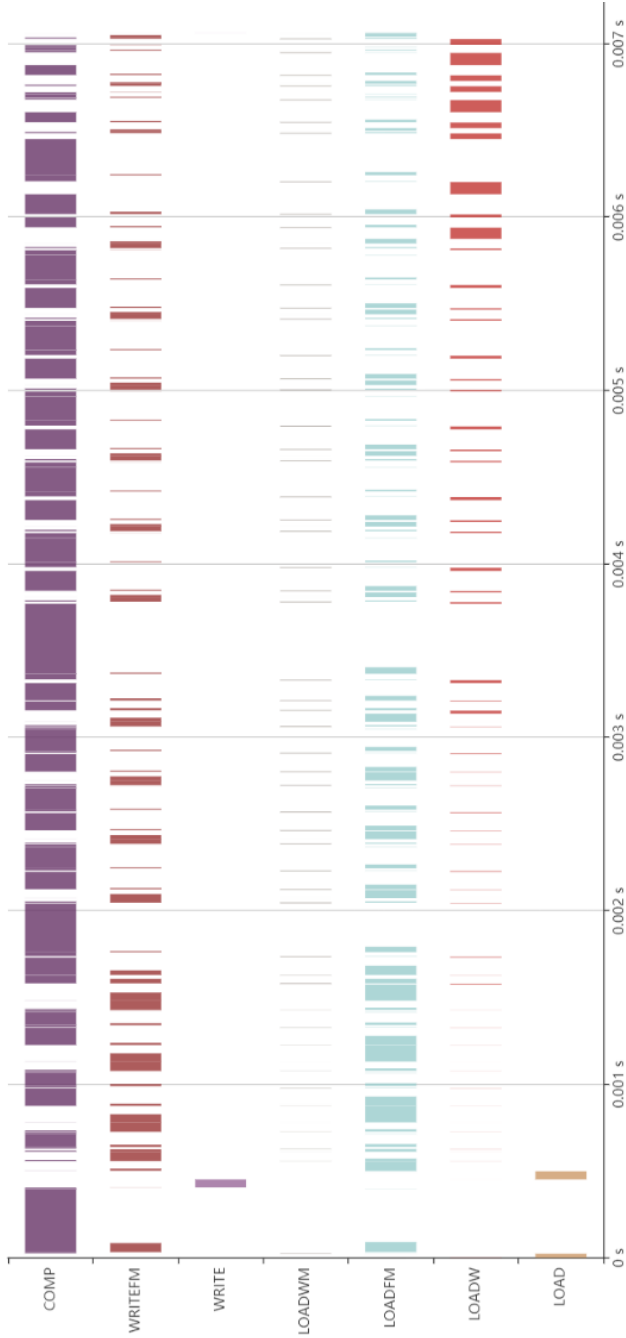


Fig. 6. Resnet50 for 4x4 AIE with 50% sparse weights

like element wise addition or concatenation). A projection  $\P$  is a function taking an output sub-tensor and projects the input sub-tensor needed to compute the output. Obviously,  $T_{j-1} + \text{Padding} = \P(L_j, T_j)$ . Consider a single  $u = 1 \times 1 = u_h \times u_w$  output at layer  $L_j$ . We consider channels immaterial and observing unitary width and height. If  $L_j$  is a convolution with kernel  $k_h \times k_w$  and stride  $s_h \times s_w$ . Then we can see that  $k_h \times k_w = k = \P(L_j, u)$  and  $s + k = \P(L_j, 2 * u)$  (simplified). For an element wise operation and a concatenation by channel, each input has  $u = \P(L_j, u)$ . This is true for different reasons.

Take the subgraph schedule and  $u_j$  as above. In reverse order, starting from  $L_j$  compute  $\P(L_j, u_j)$  and propagate the projection. When a layer  $L_m$  and tensor  $T_m$  feeds two (or more) layers  $L_x$  and  $L_y$ . Then  $u_m = \max(\P(L_x, u_x), \P(L_y, u_y))$  when  $u_x$  and  $u_y$  are defined completely and  $\max$  mean the largest. We carry the propagation of  $\P(L_m, u_m)$ . In the worst case scenario,  $T_{-1} = \P(L_0, u_0) = \prod_{l=j}^0 \P(L_l, u_l)$ , for which there is no practical advantage.

At the end of the propagation, imagine this is a generalized convolution with kernel size  $k = \P(L_0, u_0)$ . Now if we repeat the process with  $u_j = 2 \times 2 \dots k + s = \P(L_0, u_0)$ . Thus we have an estimate of the generalized stride. Now we can split the computation by selecting a non overlapping decomposition of the output tensor: say using  $M$  tiles each of size  $u_o$ . The input is split into  $M$  tiles of size  $(u_o - 1)s + k$  and we will have an overlap of size  $k - 1$ . With input overlap, thus with extra reads, we have extra computations.

### B. Live analysis and Zero DDR Communication

Assume, we have an output tile size  $u_o$ . We repeat the projection process using the schedule. This time, we keep information of the live tensors at any time in the schedule. Projections and live tensors are sufficient to represent the maximum live space requirement (not including input and output). If we want zero DDR spill, we choose a output tile for which the maximum live space is smaller than MemTile. This a simple heuristics. Say we have  $M$  tiles. With an architecture for which computation is free (see [15], [16]), we write  $T_j$  once, we read  $T_0$ , and we reread  $(M - 1)(k - 1)$ . This is better than  $\sum_{l=0}^j T_l$  especially for large  $j$ s.

A compiler can target easily a tiling with zero DDR communications. In practice, zero DDR communications is not our final goal.

### C. Iteration and Memory allocation

Take the schedule  $L_0 \dots L_j$ , let us apply the live tensor analysis and tensor projections for a specific tile size  $u_o$  and  $M$  tiles. We add two custom layers as follows

$$I_b(M), L_0, L_1, \dots, L_n, I_e(M)$$

The layer  $I_b(M)$  is an iteration layer or input boundary that takes the input tensor  $T_{-1}$  and carves out a sub-tensor shape and size  $(u_o - 1)s + k$ . The layer  $I_e(M)$  is an iteration layer or output boundary that takes the input tensor  $u_o$  and copies it to a tensor of shape and size  $T_j$ . For the purpose of the memory allocation, we have a legal schedule that describes basically the property of the computation. We can do memory allocation.

### D. Code Generation

A computation is basically defined by its layer and by the addresses in memory of its input and output tensors. The code generation unrolls the iterations as it was a loop and  $I_b$  and  $I_e$  generate the proper sub tensor addresses and specifying the number of iterations.

The code generation will be for the schedule:

$$I_b(0), L_0, L_1, \dots, L_n, I_e(0), \dots, I_b(M-1), L_0, L_1, \dots, L_n, I_e(M-1)$$

With a little of book keeping we can write the time estimates as a time series and compare performance.

### E. Complementary

The depth-wise tiling has the tendency to increase the computation number and decrease the DDR loads and stores. Sparsity reduce the number of computations and the weights communications. Together have the opportunity to work better. We present experimental evidence for VGG16 where we have the best performance when we apply both. See Section VI-B

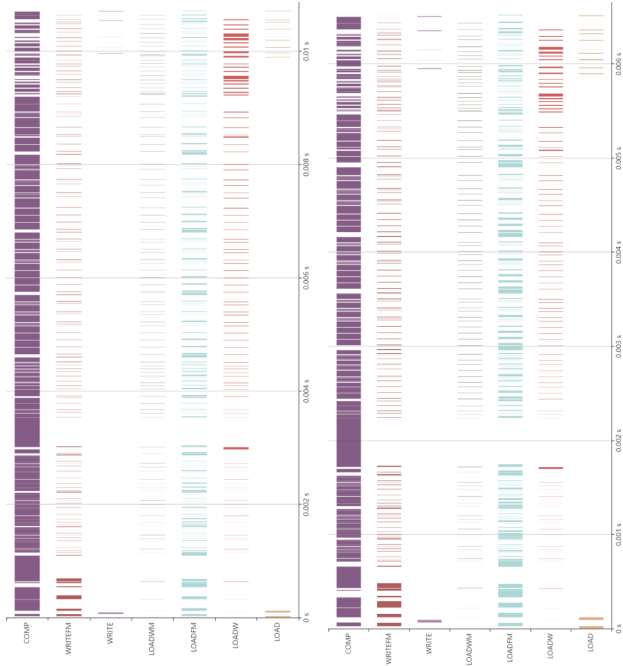


Fig. 7. Inception V3 for 6x6 AIE with dense (left/top) weights and sparse (right/bottom)

## VI. RESULTS

For presentation purpose, we split this section into two. We address first the performance of dense and sparsity overall for a set  $2 \times 2, \dots, 8 \times 8$  AIEs; second, we address the depth-wise tiling and sparsity optimizations for VGG16 and a  $3 \times 3$  AIE configuration.

### A. Results All

In this section, we present the performance of sparsity applied to all the convolutions (except the first one), see Table II, and in the appendix we present the complete set of simulation simulations, see Section VIII.

For a  $4 \times 4$  AIE setup, Resnet 50 fits in memtile from the beginning to the last operation (beside the first convolution and this is by construction). The estimates advantage by sparsity is almost completely achieved. See Figure 3 and 6.

For the estimate of Inception V3, we use a  $6 \times 6$  AIE setup. This allows a limited spill into DDR and the sparsity delivering once again an overall  $2 \times$  speed up. See Figure 7.

TABLE II  
EXECUTION TIME ESTIMATES

AIE2	Model	Dense sec	Sparse sec
2x2	Resnet	2.492347e-02	1.582626e-02
3x3		1.269543e-02	8.661490e-03
4x4		1.077318e-02	7.064918e-03
5x5		failed	4.303485e-03
6x6		5.712521e-03	4.490127e-03
7x7		4.205991e-03	3.212234e-03
8x8		6.376768e-03	4.602027e-03
2x2	IncV3	4.283837e-02	2.440544e-02
3x3		2.386600e-02	1.422390e-02
4x4		1.740967e-02	1.012540e-02
5x5		9.690552e-03	failed
6x6		1.063962e-02	6.439692e-03
7x7		8.727651e-03	failed
8x8		9.093276e-03	5.666152e-03
2x2	VGG16	4.476212e-02	2.608593e-02
3x3		failed	1.002015e-02
4x4		1.371000e-02	8.852128e-03
5x5		failed	4.336479e-03
6x6		failed	5.770197e-03
7x7		7.455440e-03	5.288551e-03
8x8		9.203393e-03	6.502333e-03

In Table II, we present the estimates of the total execution time for three networks and seven configurations. We report also the case where the compiler fails to generate code. Notice that the configuration  $8 \times 8$  is never beneficial. A full investigation is necessary.

### B. Results Depth-Wise Tiling for VGG16 3x3

We take VGG and we instruct the DDR to be 16 times slower (4GBs/16) highlighting the need of fewer DDR communications. In Figure 8, we show the performance for VGG16 until the last maxpool. In Figure 9, we highlight only the part that requires DDR spills for each layer: 0.025s. We

Fig. 8. VGG16 3x3 last Maxpool



Fig. 9. VGG16 3x3 DDR only

apply depth-wise tiling using three tiles 0.024s and we break even. With two tiles, we achieve better performance at 0.022s, see Figure 10 and 11. Sparsity by itself without any tiling can achieve only 0.021s. Sparsity and tiling improves even further and we achieve 0.014s, see Figure 12. A posteriori, we can appreciate the reduction of activation DDR communications thanks to depth-wise tiling and the reduction of computation and weights communication by sparsity.

## VII. CONCLUSIONS AND CONTEXT

This is a multifaceted problem and we present a complete solution from training techniques, compilers, code generation, HW definition, and time estimations.

This could be seen as a quantization and sparsification problem on how to reduce the footprint of a CNN network. There are post-training techniques that are targeting quantization and unstructured sparsity [17] and all the reference within and its citations. For the type of sparsity we are planning, we need to be more aggressive and trail for it (as starting point [18]). But our sparsity is not really a property of the model, it is a sparsity that the software can describe and the hardware can take advantage without having any hardware support.

Fig. 10. VGG16 3x3 DDR only 3 tiles

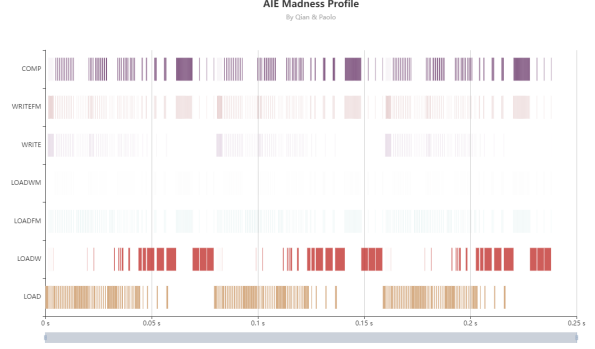


Fig. 11. VGG16 3x3 DDR only 2 tiles

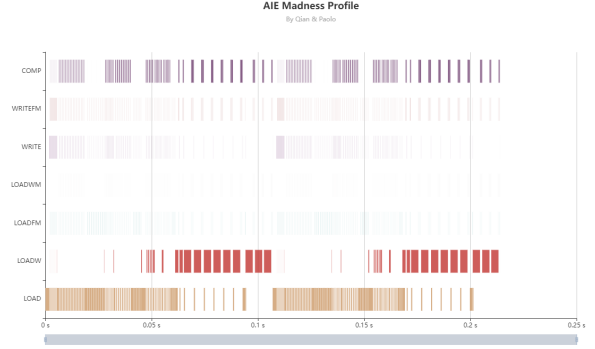
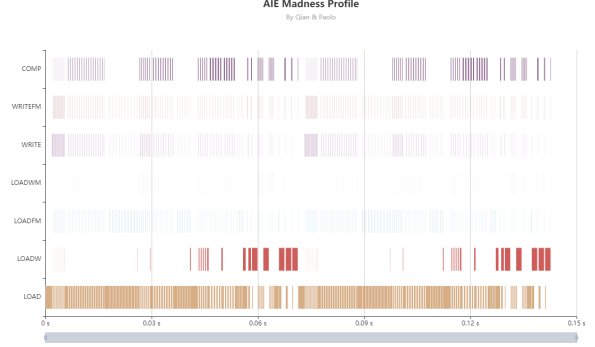


Fig. 12. VGG16 3x3 DDR only 2 tiles sparse



This work stemmed from a collaboration between Xilinx and Numenta and the idea set forward by the authors in [19], where the models are too dense and there is a lot of room for improvements. Sparsity at the beginning was proposed for weights with blocks  $4 \times 4$  and for activations (a ReLU zeros a lot and there have been prototypes programming logic was added to AIE1 fabric to support top-k run-time activations). We must thanks Vamsi Nalluri for the AIE1 prototype and the original contribution to the AIE2. With the new AIE2 and logic, the run-time support and top-k was dropped. The compiler could and can do average estimate

of tensor contents but we do not have run-time support for dynamic and unstructured sparsity. New support is coming like the 2 over 4 (4 over 8) sparsity but it is not clear how it will affect the activation encoding and total accuracy. In principle, we could use 2 by 4 zero encoding for the non-zero blocks to further reduce space and computations.

This is the second attempt to create time estimates given a specific AIE configurations. Sourabh Donfaonkar designed the first estimate model to shape the architecture and optimize the code for  $8 \times 2$  cohort row by column with two memtiles per column, within a  $8 \times 8$  shim (i.e., block), and composition of 9-10 of them. This first step investigates how split the weight by CIN and by COUT and how the random block sparsity affects the coding and actual memory foot-print (HW loves symmetric computations and unbalance computations will be reduce to balanced ones). This shaped our understanding how to compress weights. Now, we write instructions with the intent of executing them, we know where the data will be and what amount we shall move, and thus we account for most of the idiosyncrasies of the model (padding and strides) and of the communications (yes, padding).

The difficulty of generating code for complex architectures can be described and solved in different ways. There are recent attempts of introducing SW/HW solution for spatial processors like ours [20]–[22]. The main difference:

- We use software developed for FPGA custom IPs because we can reuse the two-level of memory hierarchy abstraction.
- We use heuristics to explore scheduling.
- We use heuristics to memory allocation.
  - There is a memory allocation so temporal locality is exploited and different (layer) schedules can be investigated.
  - All passes know all tensor shapes at compile time (no run-time support).
- We write *all* the data movements and the code can and is used by a AIE2 compiler (binary compiler if you like) to create executable codes.
  - Code generated for  $1 \times 1$  have been simulated, run and validated in HW.
  - We assume that core to core communication by columns (larger kernel and stride require overlapping column data) or communication by row (reduction of partial sums) are inherently taken care by the kernel computation (in practice they are not).
  - Kernel computation (the basic computation in the AIE2) has effects on the shapes and layout of the operands. The HW architects instruct the compiler about the tensor requirements.
  - The compiler does not generate fully correct addresses but all the tensor shapes are valid and correct for most  $K \times K$  of reasonable size  $K \leq 8$ .
- No full or partial simulation is needed, and now time estimates can be used to quantify scheduling and HW configurations choices. Yes, there is further arbitrary

connections and hardware configurations that can change and the effects are visible only by writing code for it ...

For simplicity, we do not provide all the details about the compiler and the AIE2 interconnections. This is a working but-in-progress software system and we intend to make it available in its entirety as much as we made public some of it.

## VIII. APPENDIX

Here, we present the collection of execution times as images:

- Figure 13 Inception V3 2x2 dense and sparse
- Figure 14 Inception V3 3x3 dense and sparse
- Figure 15 Inception V3 4x4 dense and sparse
- Figure 16 Inception V3 5x5 dense and sparse FAILs
- Figure 17 Inception V3 6x6 dense and sparse
- Figure 18 Inception V3 8x8 dense and sparse
- Figure 19 Resnet 50 2x2 dense and sparse
- Figure 20 Resnet 50 3x3 dense and sparse
- Figure 21 Resnet 50 4x4 dense and sparse
- Figure 22 Resnet 50 5x5 dense FAILs and sparse
- Figure 23 Resnet 50 6x6 dense and sparse
- Figure 24 VGG16 2x2 dense and sparse
- Figure 25 VGG16 4x4 dense and sparse
- Figure 26 VGG16 8x8 dense and sparse

## REFERENCES

- [1] AMD, “rocsparse,” <https://rocsparse.readthedocs.io/en/master/>, 2020.
- [2] NVIDIA, “cusparse,” <https://developer.nvidia.com/cusparse>, 2020.
- [3] P. D’Alberto, <https://github.com/paolodalberto/SparseFastMM/>, 2013.
- [4] F. Chollet *et al.*, “Keras,” <https://keras.io>, 2015.
- [5] P. D’Alberto, “Block sparsity and training,” <https://github.com/paolodalberto/BlockSparsityTraining>, 2020.
- [6] J. Deng, W. Dong, R. Socher, L.-J. Li, K. Li, and L. Fei-Fei, “Imagenet: A large-scale hierarchical image database,” in *2009 IEEE conference on computer vision and pattern recognition*. Ieee, 2009, pp. 248–255.
- [7] A. Paszke, S. Gross, F. Massa, A. Lerer, J. Bradbury, G. Chanan, T. Killeen, Z. Lin, N. Gimelshein, L. Antiga, A. Desmaison, A. Kopf, E. Yang, Z. DeVito, M. Raison, A. Tejani, S. Chilamkurthy, B. Steiner, L. Fang, J. Bai, and S. Chintala, “Pytorch: An imperative style, high-performance deep learning library,” in *Advances in Neural Information Processing Systems 32*, H. Wallach, H. Larochelle, A. Beygelzimer, F. d’Alché-Buc, E. Fox, and R. Garnett, Eds. Curran Associates, Inc., 2019, pp. 8026–8037. [Online]. Available: <http://papers.nips.cc/paper/9015-pytorch-an-imperative-style-high-performance-deep-learning-library.pdf>
- [8] Z. Yao, A. Gholami, S. Shen, K. Keutzer, and M. W. Mahoney, “Adahessian: An adaptive second order optimizer for machine learning,” *AAAI (Accepted)*, 2021.
- [9] S. Yu, Z. Yao, A. Gholami, Z. Dong, M. W. Mahoney, and K. Keutzer, “Hessian-aware pruning and optimal neural implant,” *CoRR*, vol. abs/2101.08940, 2021. [Online]. Available: <https://arxiv.org/abs/2101.08940>
- [10] B. Zandonati, A. A. Pol, M. Pierini, O. Sirkin, and T. Kopetz, “Fit: A metric for model sensitivity,” 2022.
- [11] Y. Jia, E. Shelhamer, J. Donahue, S. Karayev, J. Long, R. Girshick, S. Guadarrama, and T. Darrell, “Caffe: Convolutional architecture for fast feature embedding,” in *Proceedings of the 22nd ACM International Conference on Multimedia*, ser. MM ’14. New York, NY, USA: Association for Computing Machinery, 2014, p. 675–678. [Online]. Available: <https://doi.org/10.1145/2647868.2654889>
- [12] TensorFlow. [Online]. Available: <https://www.tensorflow.org/>
- [13] P. D’Alberto, V. Wu, A. Ng, R. Nimaiyar, E. Delaye, and A. Sirasao, “Xdn: Inference for deep convolutional neural networks,” *ACM Trans. Reconfigurable Technol. Syst.*, vol. 15, no. 2, jan 2022. [Online]. Available: <https://doi.org/10.1145/3473334>
- [14] P. D’Alberto, J. Ma, J. Li, Y. Hu, M. Bollavaram, and S. Fang, “DPUV3INT8: A compiler view to programmable FPGA inference engines,” *CoRR*, vol. abs/2110.04327, 2021. [Online]. Available: <https://arxiv.org/abs/2110.04327>
- [15] J.-W. Hong and H. T. Kung, “I/o complexity: The red-blue pebble game,” in *Symposium on the Theory of Computing*, 1981. [Online]. Available: <https://api.semanticscholar.org/CorpusID:8410593>
- [16] G. Bilardi, A. Pietracaprina, and P. D’Alberto, “On the space and access complexity of computation dags,” in *Graph-Theoretic Concepts in Computer Science, 26th International Workshop, WG 2000, Konstanz, Germany, June 15-17, 2000, Proceedings*, ser. Lecture Notes in Computer Science, U. Brandes and D. Wagner, Eds., vol. 1928. Springer, 2000, pp. 47–58. [Online]. Available: [https://doi.org/10.1007/3-540-40064-8\\_6](https://doi.org/10.1007/3-540-40064-8_6)
- [17] E. Frantar, S. Ashkboos, T. Hoefler, and D. Alistarh, “Gptq: Accurate post-training quantization for generative pre-trained transformers,” 2023.
- [18] B. Hawks, J. M. Duarte, N. J. Fraser, A. Pappalardo, N. Tran, and Y. Umuroglu, “Ps and qs: Quantization-aware pruning for efficient low latency neural network inference,” *CoRR*, vol. abs/2102.11289, 2021. [Online]. Available: <https://arxiv.org/abs/2102.11289>
- [19] S. Ahmad and L. Scheinkman, “How can we be so dense? the benefits of using highly sparse representations,” 2019.
- [20] Q. Huang, M. Kang, G. Dinh, T. Norell, A. Kalaiah, J. Demmel, J. Wawrzyniek, and Y. S. Shao, “Cosa: Scheduling by constrained optimization for spatial accelerators,” *2021 ACM/IEEE 48th Annual International Symposium on Computer Architecture (ISCA)*, pp. 554–566, 2021. [Online]. Available: <https://api.semanticscholar.org/CorpusID:233740109>
- [21] E. Russo, M. Palesi, G. Ascia, D. Patti, S. Monteleone, and V. Catania, “Memory-aware dnn algorithm-hardware mapping via integer linear programming,” *Proceedings of the 20th ACM International Conference on Computing Frontiers*, 2023. [Online]. Available: <https://api.semanticscholar.org/CorpusID:260442361>
- [22] J. Cai, Y. Wei, Z. Wu, S. Peng, and K. Ma, “Inter-layer scheduling space definition and exploration for tiled accelerators,” *Proceedings of the 50th Annual International Symposium on Computer Architecture*, 2023. [Online]. Available: <https://api.semanticscholar.org/CorpusID:259177591>



Fig. 13. Inception for 2x2 AIE with dense (left/top) weights and sparse (right/bottom)



Fig. 14. Inception for 3x3 AIE with dense (left/top) weights and sparse (right/bottom)





Fig. 15. Inception for 4x4 AIE with dense (left/top) weights and sparse (right/bottom)

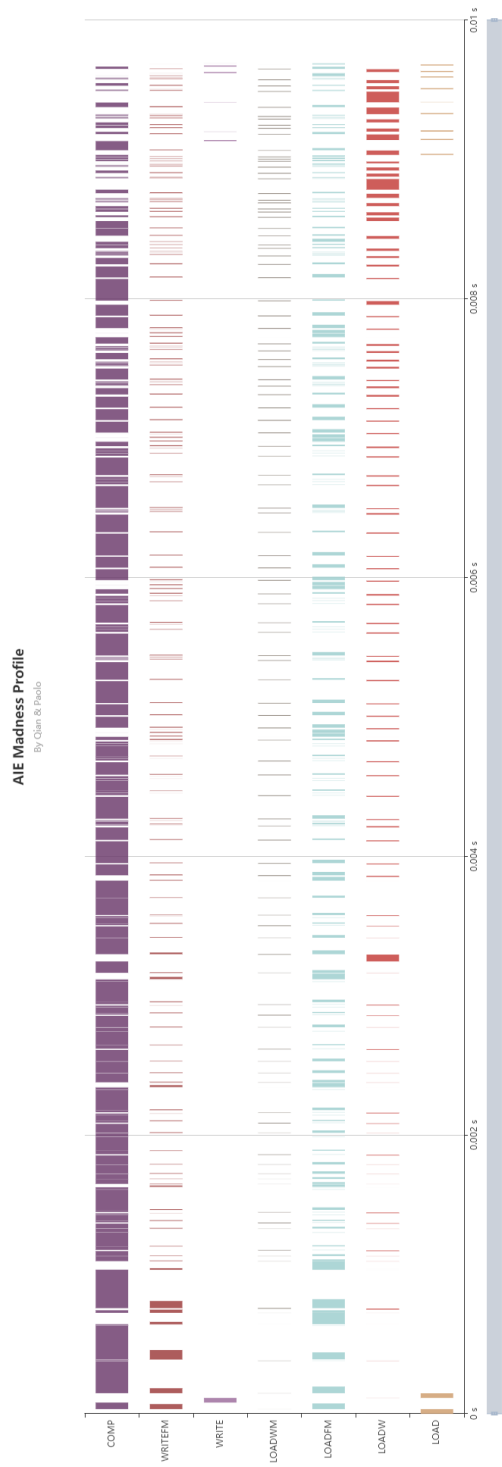


Fig. 16. Inception for 5x5 AIE with dense weights and FAILED for sparse weights

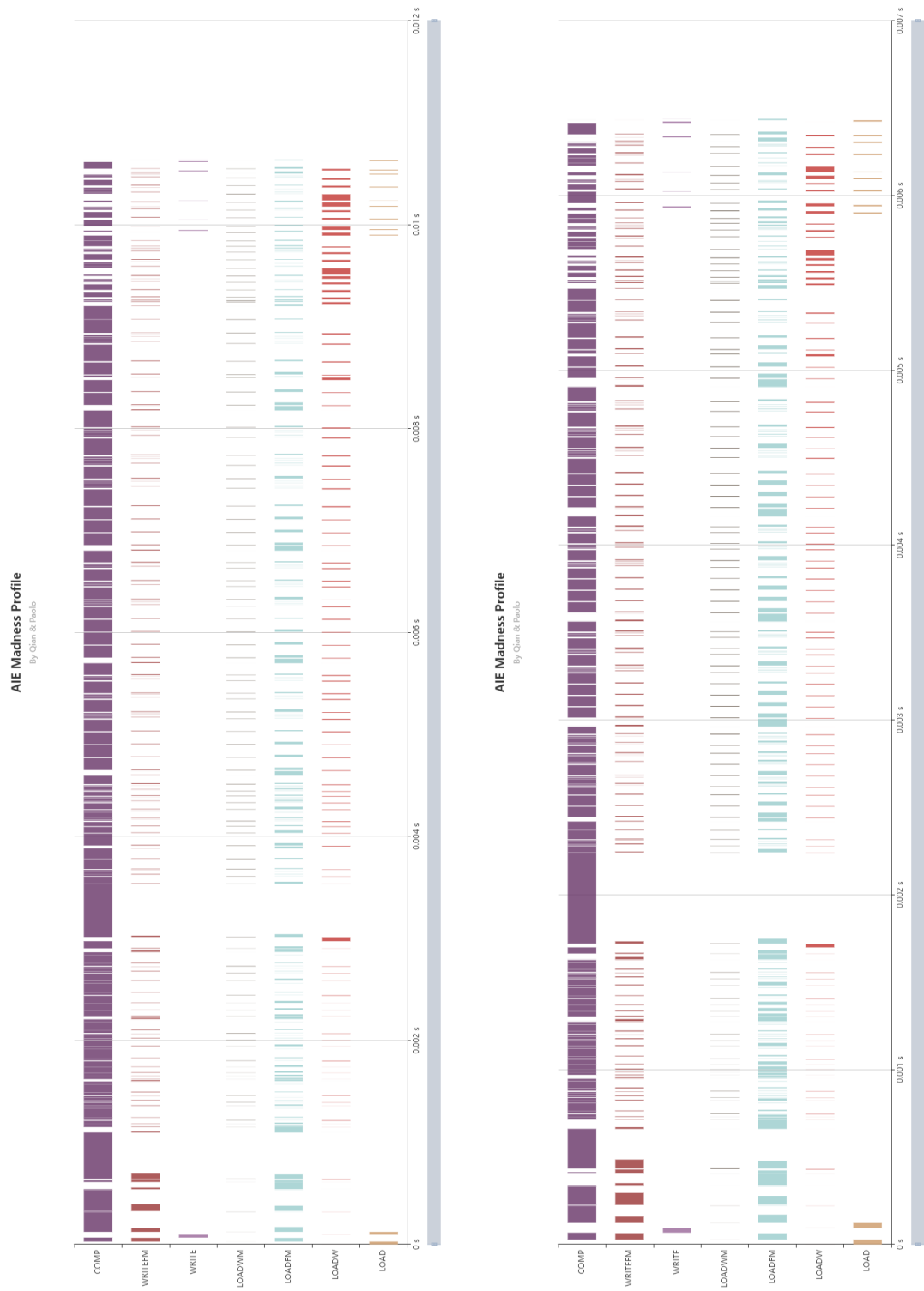


Fig. 17. Inception for 6x6 AIE with dense (left/top) weights and sparse (right/bottom)



Fig. 18. Inception for 8x8 AIE with dense (left/top) weights and sparse (right/bottom)

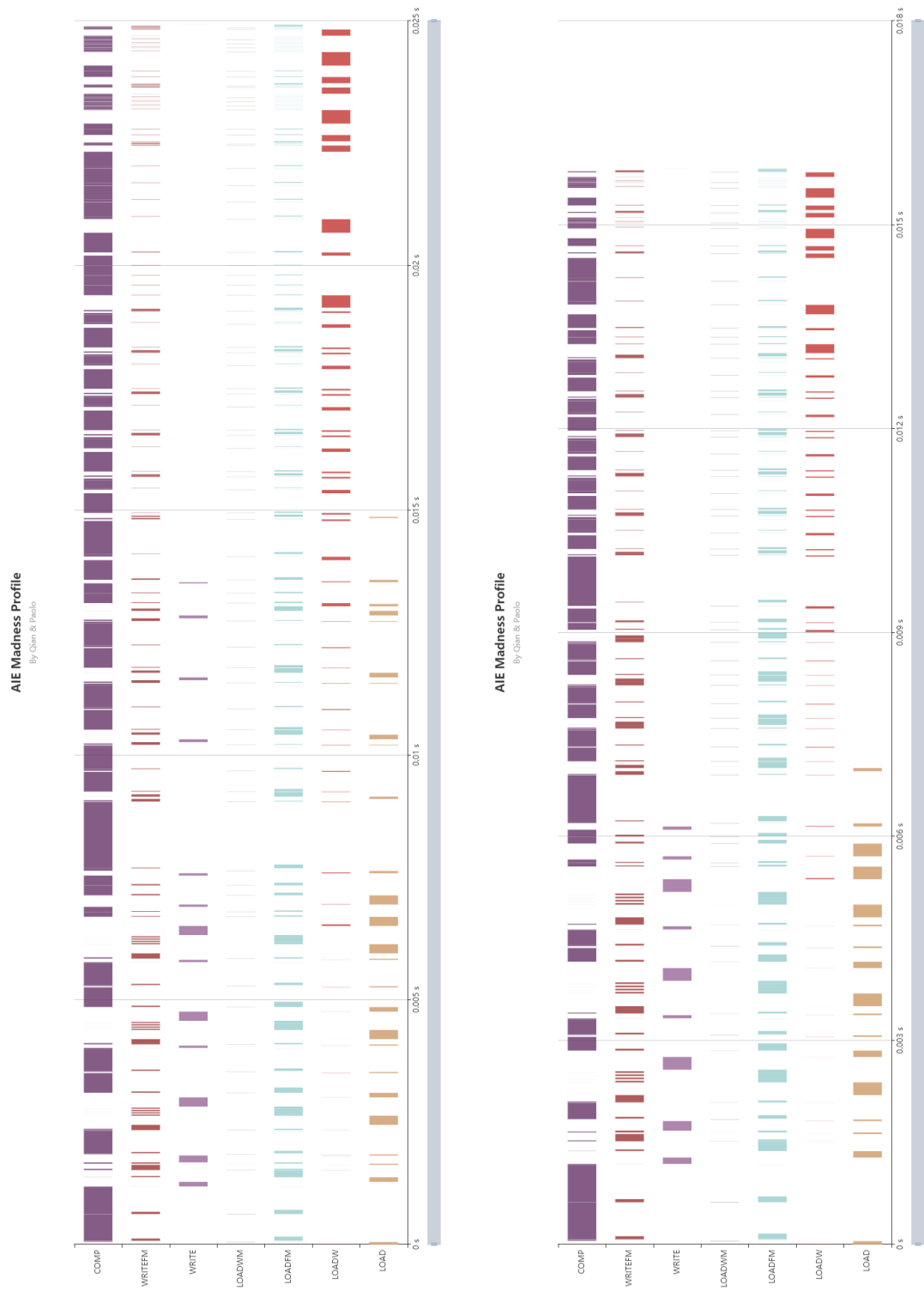


Fig. 19. Resnet for 2x2 AIE with dense (left/top) weights and sparse (right/bottom)



Fig. 20. Resnet for 3x3 AIE with dense (left/top) weights and sparse (right/bottom)

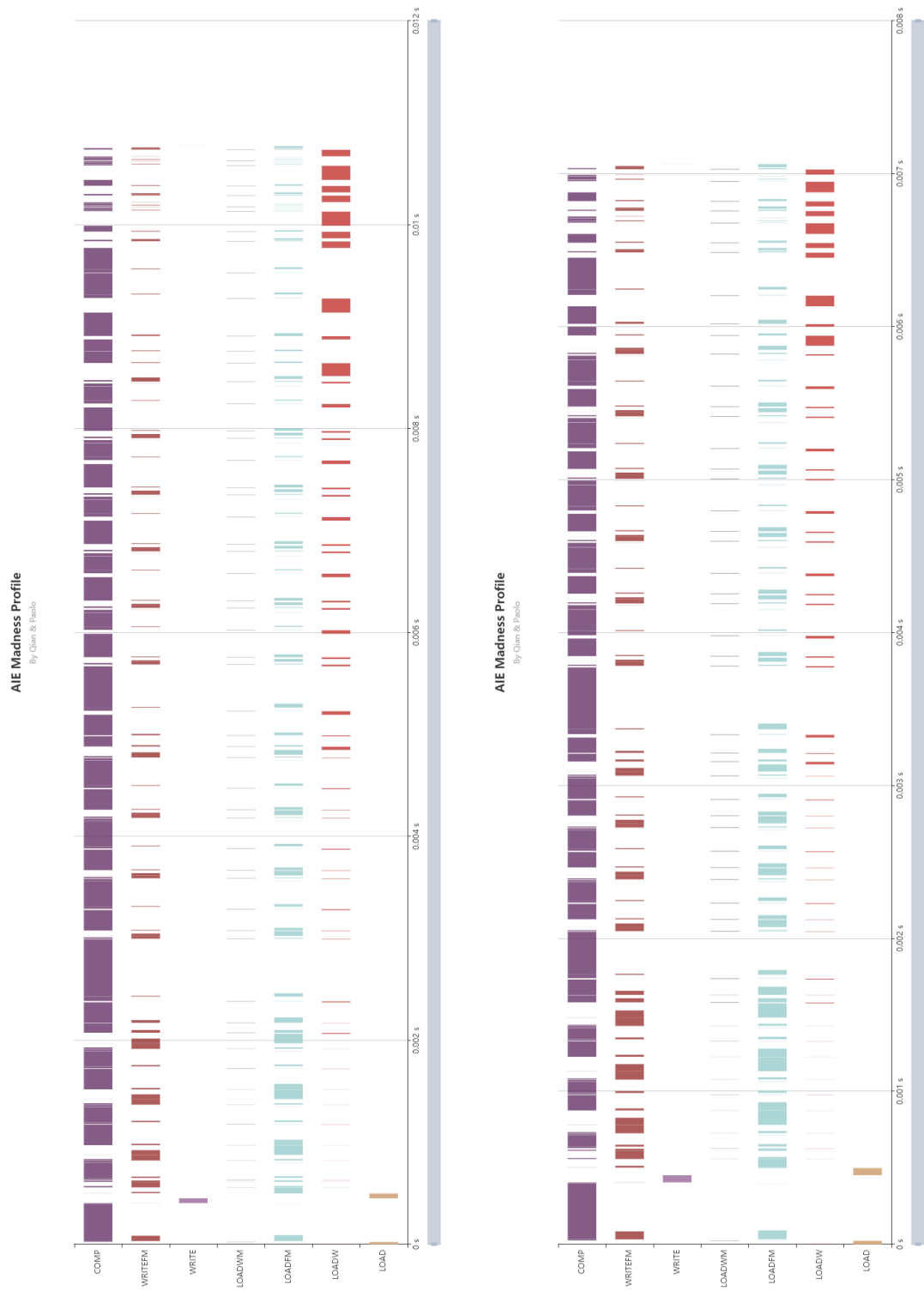


Fig. 21. Resnet for 4x4 AIE with dense (left/top) weights and sparse (right/bottom)



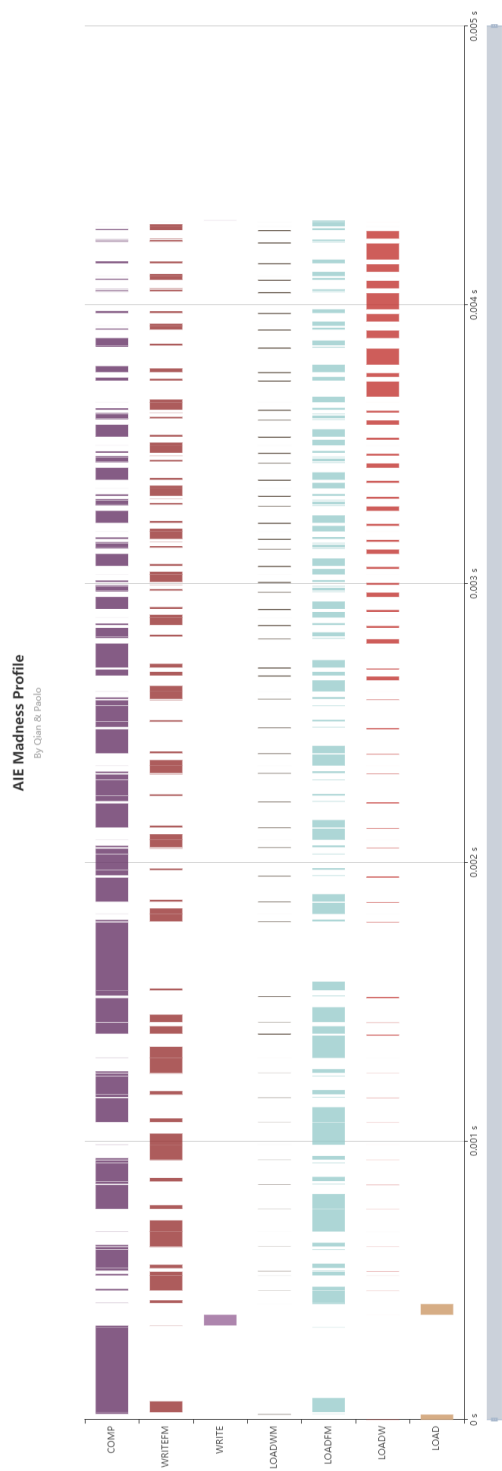


Fig. 22. Resnet for 5x5 AIE with sparse weights and FAILED for dense weights

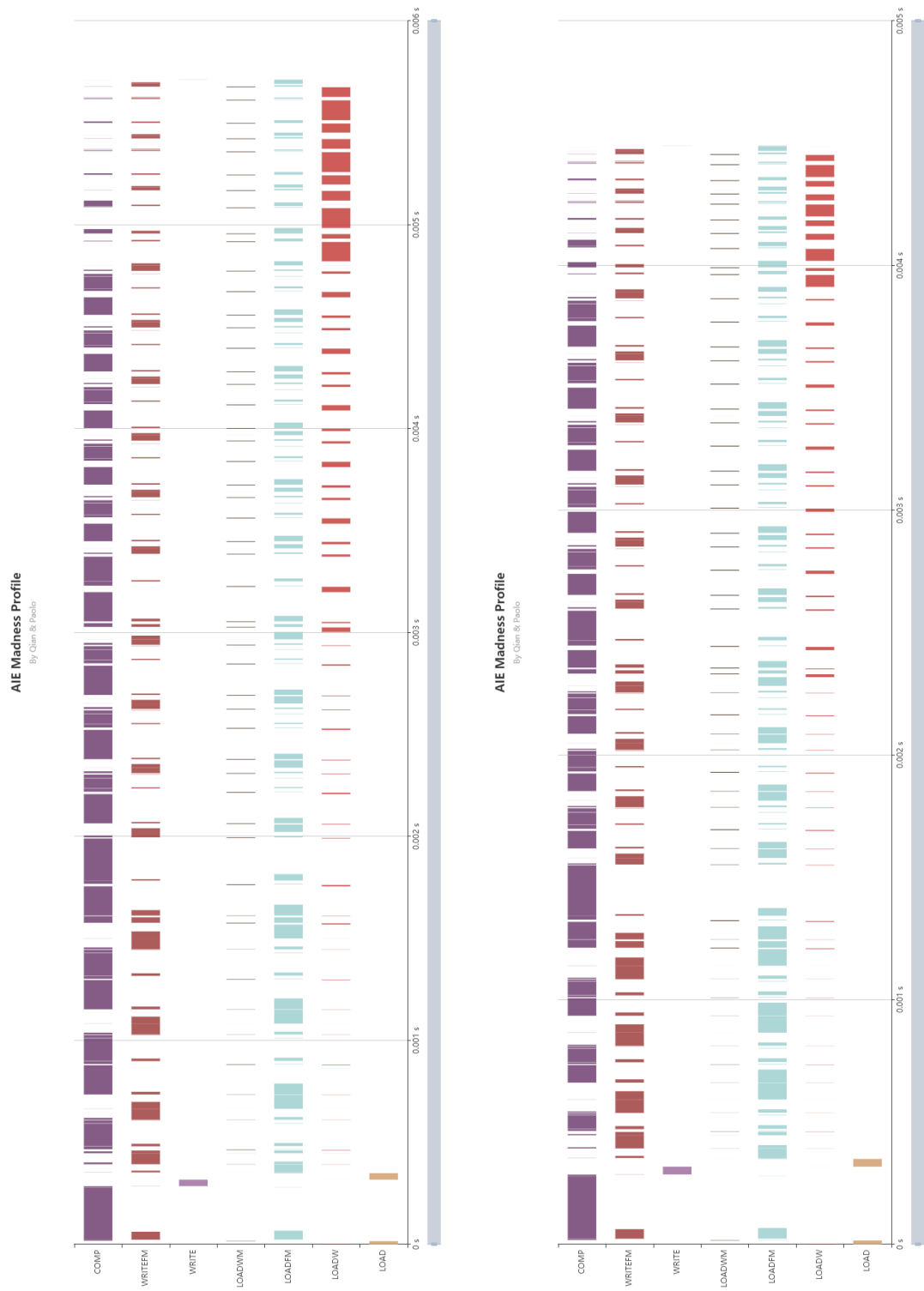


Fig. 23. Resnet for 6x6 AIE with dense (left/top) weights and sparse (right/bottom)

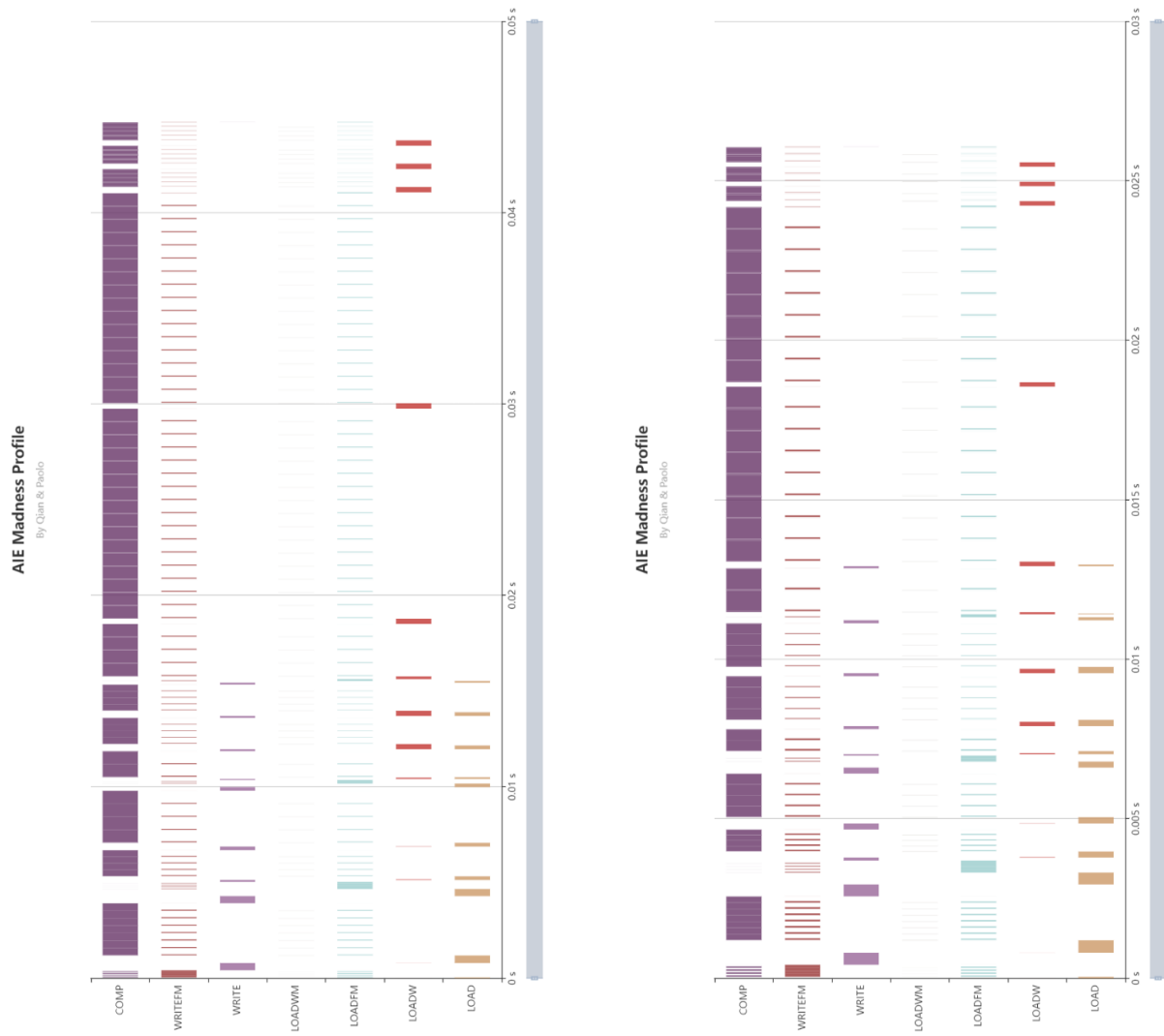


Fig. 24. VGG 16 (No FC) for 2x2 AIE with dense (left/top) weights and sparse (right/bottom)

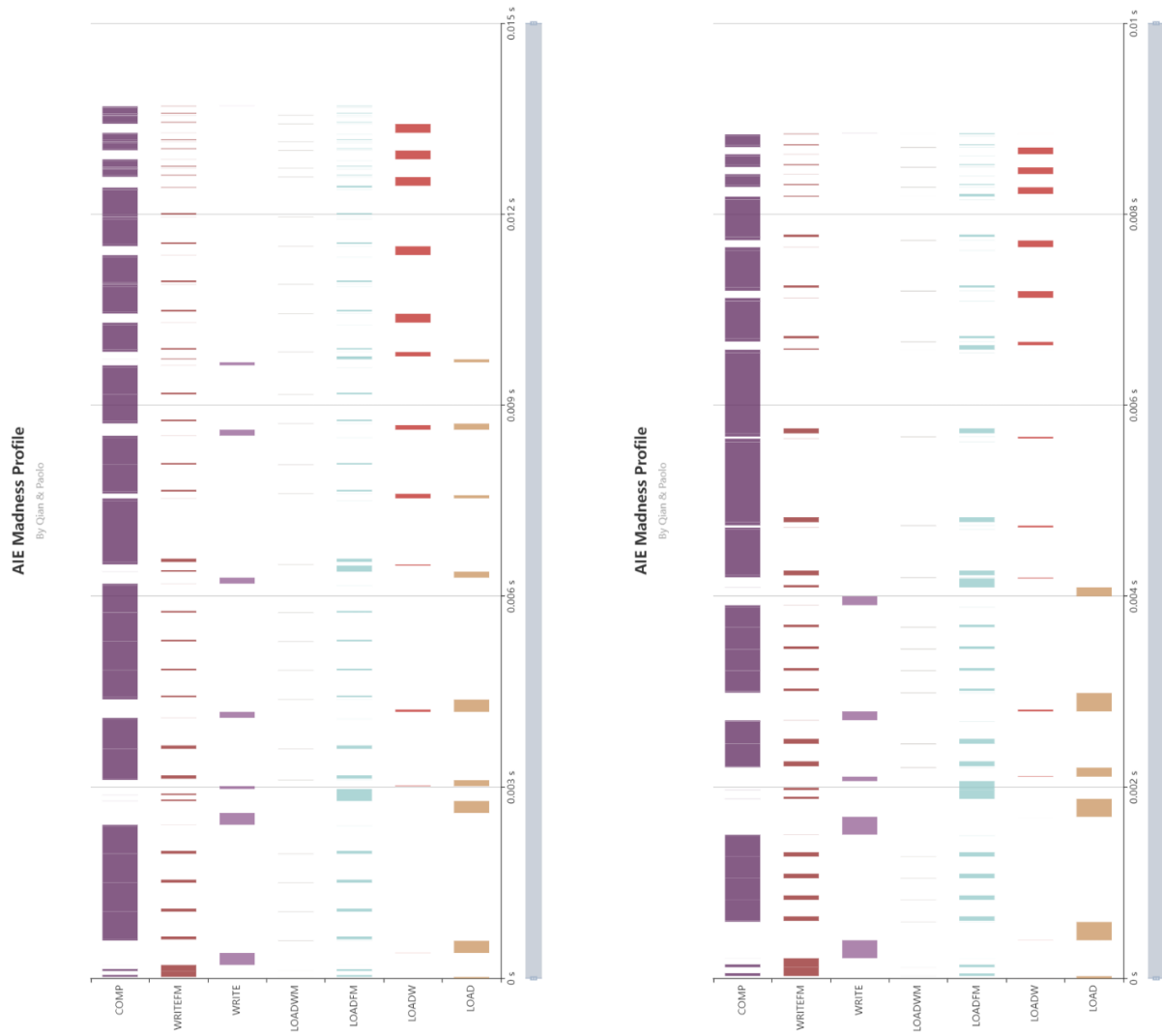


Fig. 25. VGG 16 (No FC) for 4x4 AIE with dense (left/top) weights and sparse (right/bottom)

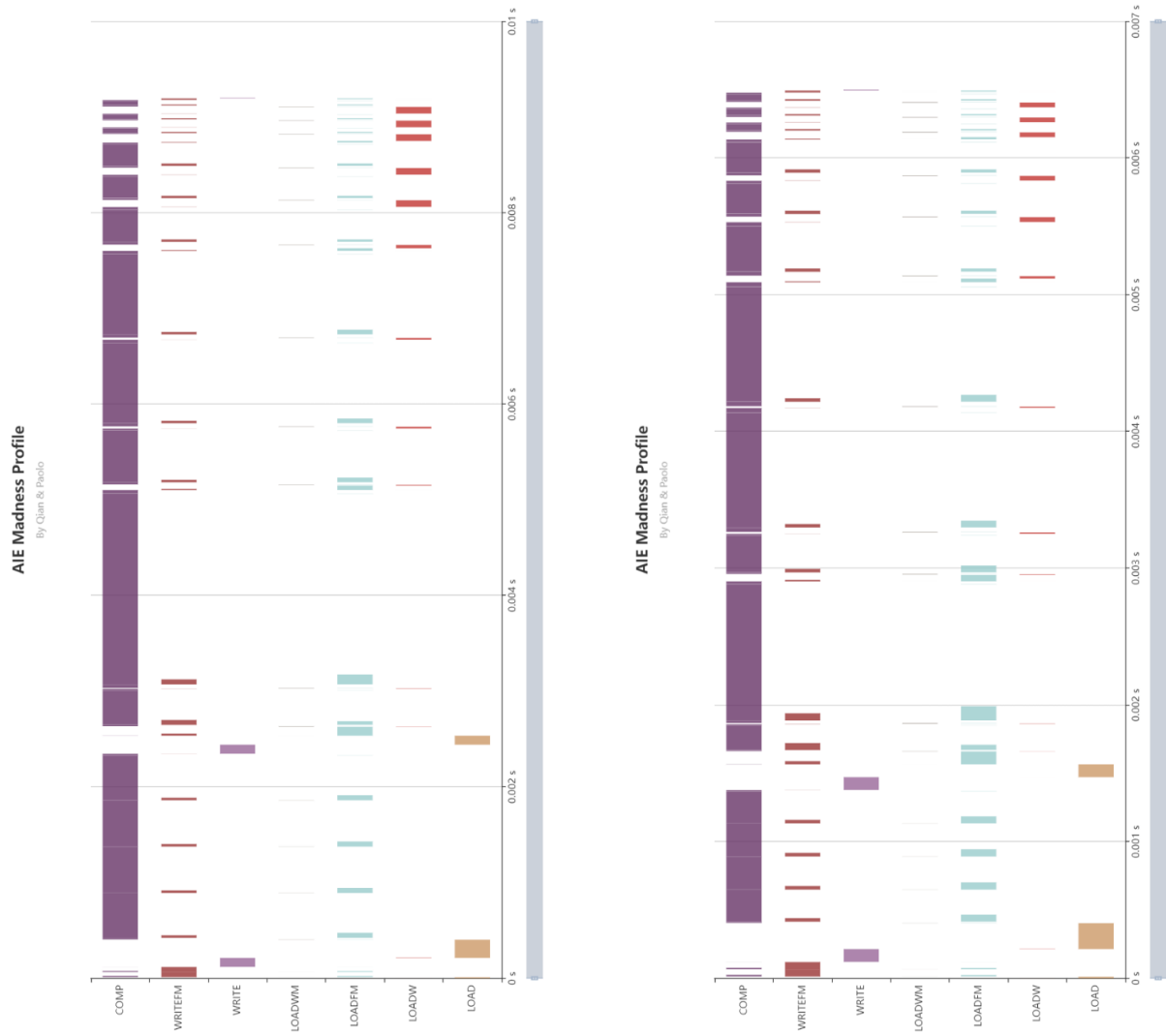


Fig. 26. VGG 16 (No FC) for 8x8 AIE with dense (left/top) weights and sparse (right/bottom)